JOURNAL OF THERMOPHYSICS AND HEAT TRANSFER
Vol. , No. ,

Anisotropic Thermal Diffusivity Measurement Using the Flash Method

Robert L. McMasters*
Virginia Military Institute, Lexington, Virginia 24450
and
Ralph B. Dinwiddie†
Oak Ridge National Laboratory, Oak Ridge, Tennessee 37831

DOI: 10.2514/1.T4189

A well-established method for determining the thermal diffusivity of materials is the laser flash method. The work presented here compares two analysis methods for flash heating tests on anisotropic carbon bonded carbon fiber. This material exhibits a higher conductivity in the direction in which the fibers are oriented than in the direction perpendicular to the fiber orientation. Of the two analysis methods used, one method uses the temperature data from the entire surface of the sample by examining 201 temperature histories simultaneously, with each temperature history originating from an individual pixel within a line across the middle of the sample. The other analysis method uses only the temperature history from a single pixel in the center of the sample, similar to the data that is traditionally generated using the classical flash diffusivity method. Both analysis methods include accommodations for modeling the penetration of the laser flash into the porous surface of the carbon bonded carbon fiber material. The robustness of the method using the single-pixel temperature history shows that anisotropic thermal diffusivity can be measured using standard flash diffusivity instruments, if modeled properly, avoiding the additional complexity associated with the use of a thermal imaging camera.

Nomenclature

a	=	mean free path of photon in porous material, m
Bi	=	Biot number (dimensionless)
c	=	specific heat, $\mathrm{J/kg-K}$
h	=	convection coefficient, $\mathrm{W/m^2\,K}$
i	=	counting integer
k_a	=	axial thermal conductivity, $\mathrm{W/m\,K}$
k_r	=	radial thermal conductivity, $\mathrm{W/m\,K}$
L	=	thickness of sample, m
m	=	counting integer for infinite series solution
n	=	number of temperature measurements
p	=	number of parameters
q_o	=	magnitude of flash, $\mathrm{J/m^2}$
$q_o/\rho cL$	=	heat pulse magnitude
r	=	radial dimension variable, m
r_h	=	heated radius of sample, m
r_o	=	outer radius of sample, m
T	=	calculated temperature in sample, K
t	=	time variable, s
x	=	spatial variable in the axial direction, m
Y	=	measured temperature in sample above ambient, K

Greek

α	=	thermal diffusivity, $\mathrm{m^2/s}$
α_a	=	axial thermal diffusivity, $\mathrm{m^2/s}$
α_r	=	radial thermal diffusivity, $\mathrm{m^2/s}$
Δr	=	radial finite difference length, m
Δx	=	axial finite difference length, m
ρ	=	density, $\mathrm{kg/m^3}$
σ	=	standard deviation of residuals, K

Received 8 May 2013; revision received 21 March 2014; accepted for publication 21 March 2014; published online XX epubMonth XXXX.

*Department of Mechanical Engineering; mcmastersrl@vmi.edu.
†High Temperature Materials Laboratory; dinwiddierb@ornl.gov.

I. Introduction

A COMMON procedure for determining thermal diffusivity is the laser flash method. Mathematical models used in the analysis of the data from the first experiments performed, using the flash method, were reasonably simple. The primary assumptions in these models included a negligibly short flash duration, surface heating of the sample, and thermal properties that were isotropic [1]. In many cases, negligible convection from the surface was also assumed. As computing power has grown over the years, the mathematical models used in the analysis of these experiments have become increasingly sophisticated. Further development of flash diffusivity experiments by Cowan [2] added tabulated heat loss correction factors to bring about refinements in the basic method used by Parker et al. [1]. The user in this instance would enter charts with properties such as surface emissivity, ambient temperature, and peak sample temperature. This work was further expanded by Clark and Taylor [3] to include heat losses from the sample circumference, which accounts for some of the effects of two-dimensional (2-D) heat transfer in the experiment. Subsequent work further improved the analysis of flash diffusivity experiments using the principle of nonlinear regression via least squares. This feature allows the mathematical model to adapt to the experimental measurements in these types of experiments. Koski [4] performed some of the initial work in this area and this was further expanded by Taylor [5].

Some of the advantages of the flash method for determining thermal diffusivity include the simplicity of the experimental setup and the small size of the samples required. Additionally, the short duration of the procedure allows redundancy of the experimental results through the rapid replication of experiments. However, the use of the flash method for determining anisotropic properties has not been exploited in routine practice. Other methods that have been used in determining anisotropic properties include a method involving multiple temperature histories. This method is discussed by Amazouz et al. [6] in using the method of moments to analyze the temperature histories recorded from locations at prescribed intervals on the sample. Another analysis made use of a mathematical model that used the ratios of temperatures measured at various locations. This method is discussed by Graham et al. [7].

A survey paper by Cernuschi et al. [8] covers several methods of thermal diffusivity measurement used over the years. The classical Parker [1] method is described there, as well as thermal wave interferometry, which makes use of an oscillating heat source, measuring phase shift to calculate thermal properties. There are also four thermographic methods discussed and compared in this work, some of which involve oscillatory heating and others that involve flash heating. All cases addressed in [8] involve isotropic materials. However, Kruczek et al. [9] address anisotropic cases for measurements in samples that are large enough to be considered semi-infinite with one planar face. A pulse is applied to one point on the face and isotherms are fitted to a mathematical model. The model assumes that the surface is adiabatic, with the exception of the instantaneous pulse. Czichos et al. [10] provide an overview of various kinds of material properties, including mechanical, electrical, optical, and thermal properties, among others. The flash method of diffusivity measurement is mentioned in this collection for isotropic materials. Dealing with anisotropic properties is addressed in this reference as it pertains generally to mathematical modeling and parameter estimation.

Of the references previously listed, [9] is the closest to the work discussed here. Some of the differences include the fact that convection is modeled in the present work, which is important in high-temperature applications, and the samples can be tested in standard flash diffusivity measurement systems, which are fairly ubiquitous. With this method, the need to relocate the flash heating device in order to record temperatures with the thermal camera is eliminated, which is advantageous for measuring high-conductivity materials. The results discussed in this work allow data from a typical single-point-measurement flash diffusivity system to be analyzed to determine orthotropic properties, simplifying both the experimental setup and the analysis phase of the work. One advantage of the method used in [9] is that directional diffusivity can be measured in two directions in the plane parallel to the surface of the material, whereas the present method assumes the in-plane diffusivity to be uniform.

Four mathematical models are compared in this research in order to account for physical effects in the experiment that, if left unaccounted for, result in a statistically significant variation in the conformance of the model to the experimental measurements. Additionally, a comparison of two measurement methods is developed as part of the present research. The comparison involves two analyses of the same type of flash diffusivity experiment. The first analysis method uses only one temperature history measured at the center of the sample. The second analysis method makes use of a full-width set of 201 temperature histories across the entire nonheated side of the sample. In the execution of both of these methods, the measurements were made with a thermal camera with a recording rate of 60 Hz. For the analysis method involving only one temperature history, the temperatures were obtained from a single pixel in the center of the sample.

For the analysis method involving multiple temperature histories, a line of pixels was used across the back of the sample so that the entire surface of transient temperatures could be mapped, taking advantage of the radial symmetry of the sample. One of the main objectives of the work was to verify the viability of an anisotropic parameter estimation method involving only one temperature history at the center of the sample. Because conventional flash diffusivity instruments use only one temperature history, it would be convenient to use this well-established method in determining anisotropic thermal diffusivity, avoiding the expense and complexity associated with 2-D transient temperature measurement and analysis.

II. Description of Experiment

Experiments were performed at the Thermo-physical Properties User Center at the High Temperature Materials Laboratory at the Oak Ridge National Laboratory. The flash diffusivity instrument used was a model Acute 2-2400 xenon flash unit manufactured by ProPhoto. The rated maximum energy of this flash device is 2400 J, which was the power level used in all experiments, and was deposited over a 3 ms duration. The sample thickness was 2.52 mm and the sample diameter was 12.57 mm. The sample used in the experiment was a carbon bonded carbon fiber (CBCF) material that typically exhibits

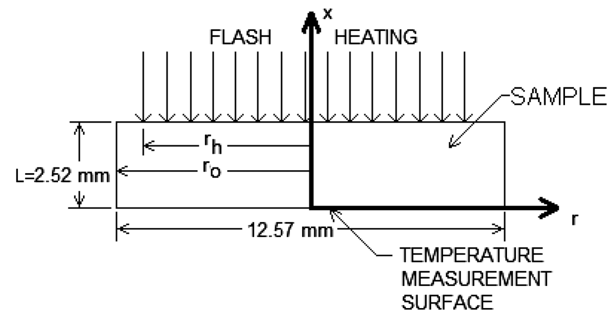

Fig. 1 Schematic diagram of disc-shaped sample in experimental setup.

anisotropic thermal properties because of the orientation of the fibers. The flash heating for the thermal diffusivity tests is applied to one such surface, and transient temperatures are subsequently measured with a thermal camera on the opposite surface. The instrument used was an Indigo Phoenix Midwave IR camera, with an InSb snapshot focal plane array with 320 by 256 pixels. The term snapshot refers to the fact that all pixels at a given time step are captured at the same time and for the same length of time. Then they are read out of the camera sequentially. Figure 1 shows a schematic diagram of the experiment as a side view of the disc-shaped sample. The rated spatial resolution of the camera is 0.1 mm and the minimum detectable temperature rise is 0.015°C. However, the standard deviation of the temperatures prior to the initiation of the flash heating was 0.051°C, which gives an estimate of the magnitude of the measurement errors.

Figure 2 shows the temperature history from a single point on the nonheated side of the sample, along with a plot of the basic mathematical model for the problem assuming isotropic properties and no penetration of the flash. More detail about the model is given in Sec. III. As can be seen in this figure, there is a discrepancy between the experimental temperature history and the mathematical model. Detailed information about the magnitude of this error is given in Sec. IV.

During the synthesis of this material, carbon fibers are suspended in a carbon slurry and are then pressed at high pressure and cured. Through this process, the fibers tend to align themselves in a direction perpendicular to the applied compression force. As such, the thermal conductivity is typically greater along the axis of the fibers than perpendicular to the fibers. This causes the material to exhibit anisotropic thermal properties. Specifically, the material is expected to exhibit orthotropic conductivity because of the uniform alignment of the fibers parallel with the surface and perpendicular to the direction of heat flow during the experiment. The orthotropic properties exhibited by the material are desirable for thermal protection systems in automotive and aerospace applications, among others. In many of these cases, it is advantageous to conduct heat along the axis parallel to the surface in order to dissipate localized high-temperature areas. At the same time, it is also desirable to present a boundary of low thermal conductivity perpendicular to the

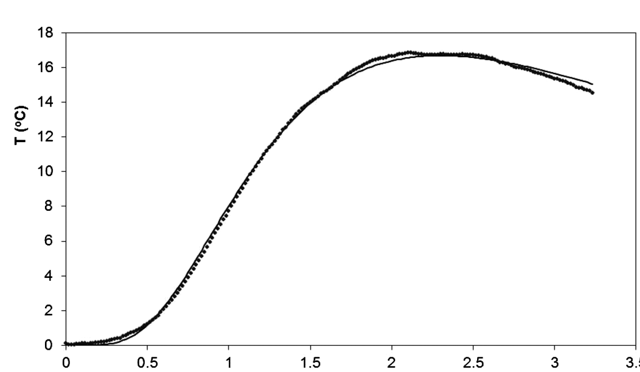

Fig. 2 Temperature history lines from nonheated side of sample. The mathematical model is shown as a continuous line and the temperature measurements are shown as individual points.

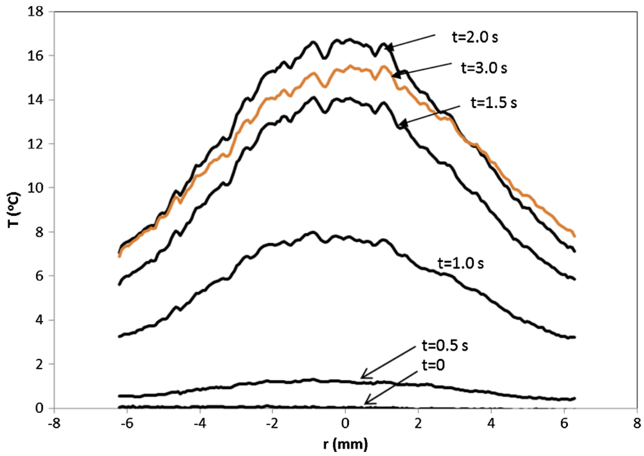

Fig. 3 Selected temperature history lines from nonheated side of sample.

surface of the material. The CBCF material was manufactured at the Oak Ridge National Laboratory and was developed at the lab for insulation used in radioisotope thermoelectric generators for deep space missions such as Voyager, Galileo, Cassini, and the Apollo lunar landing missions.

Figure 3 shows a collection of selected temperatures measured across the nonheated side of the sample, expressed in terms of the temperature rise above ambient temperature. As can be seen in this figure, the temperature increases slightly at a time of 0.5 s and continues to rise until a time of approximately 2 s. The temperature is highest in the center, mainly due to the heat loss around the perimeter of the disc-shaped sample.

Another factor affecting the temperature distribution is the center weighting of the heating of the sample. Ideally, the heating is intended to be uniform across the sample surface, however a feature was added to the mathematical model used in this research to accommodate nonuniform center-weighted heating, and an improved fit was found using this feature. To accomplish this, a parameter corresponding to the heated radius r_h was added to the model and was allowed to be optimized as part of the process of conforming the mathematical model to experimental measurements. Overall, three sets of experiments were conducted and the results were all very similar, normally within a few percentage points of each other.

III. Analysis Method

A 2-D numerical solution was developed for the cylindrical (disc-shaped) sample to be used as the direct solution in the parameter estimation scheme. The differential equation being solved in this anisotropic analysis is

$$\rho c \frac{\partial T}{\partial t} = k_a \frac{\partial^2 T}{\partial x^2} + \frac{k_r}{r} \frac{\partial}{\partial r}\left(r \frac{\partial T}{\partial r} \right) \tag{1}$$

where k_a is the thermal conductivity in the axial direction $(\mathrm{W/m-K})$, k_r is the thermal conductivity in the radial direction $(\mathrm{W/m-K})$, and ρc is volumetric heat capacity $(\mathrm{J/m^3})$. The boundary conditions subsequent to the flash are

$$k_a \frac{\partial T}{\partial x}\bigg|_{x=0} = hT(r, 0, t) \tag{2}$$

$$-k_a \frac{\partial T}{\partial x}\bigg|_{x=L} = hT(r, L, t) \tag{3}$$

$$-k_r \frac{\partial T}{\partial r}\bigg|_{r=r_o} = hT(r_o, x, t) \tag{4}$$

In these equations, h is the convection coefficient $(\mathrm{W/m^2\,K})$, T_∞ is the ambient temperature (K), and r_o is the outer radius of the sample. The flash heating is modeled as an initial condition and a detailed description of the various types of initial conditions are given in Table 1, as well as Eqs. (5) and (6) next. For the simplest model used in this analysis, the heating was assumed to have taken place only on the surface, and so the initial condition involved an elevated temperature at $t = 0$ on the surface nodes in the numerical solution. The numerical solution was a finite control volume scheme arranged so that temperatures could be computed for each of the pixels measured by the thermal camera on the surface. The number of nodes in the axial direction in the sample is 10. The recording frequency of the thermal camera was 60 Hz, but the time steps in the numerical solution were established so that they would not exceed a dimensionless value of 0.05 based on the node spacing and diffusivity in either direction (i.e., $\alpha_a t/\Delta x^2$ or $\alpha_r t/\Delta r^2$, where Δx and Δr are the finite difference lengths for the axial and radial directions, respectively).

As part of the analysis of the single-point measurement method, four mathematical models were compared in terms of their adequacy in fitting the experimental measurements. The four models are summarized in Table 1, including the model designation (a, b, c, d), a description of the model, and the parameters included in the model.

As part of the more sophisticated initial conditions, two special surface heating features are modeled. One is that the heated diameter of the sample surface is different from the overall diameter of the sample. The flash intensity is considered uniform over the heated surface but only part of the incident surface is heated from $r = 0$ to $r = r_h$. The second special feature involves the penetration of the flash into the material beyond the actual heated surface. This feature of the model accounts for the porosity of the material, which causes much of the flash energy to be deposited inside the sample [11]. The initial condition in this axial dimension assumes a decaying exponential distribution of energy beyond the heated surface as a function of the axial dimensional variable x. The initial conditions can be written as

$$\begin{aligned} T(r > r_h, x, 0) &= 0 \\ T(r \le r_h, x, 0) &= \frac{q_o}{\rho c a} e^{-x/a} \end{aligned} \tag{5}$$

where r_h is the radius (m) of the sample surface that is heated, a is the mean free path of a photon in the material (m), ρ is density $(\mathrm{kg/m^3})$, c is specific heat $(\mathrm{J/kg\,K})$, and q_o is the amount of heat absorbed $(\mathrm{J/m^2})$ from the flash. The parameter q_o must be calculated in order to establish the initial condition, but is not desired as part of the objective of the experiment. It is therefore considered a throwaway parameter. This parameter is used in the expression

$$\frac{q_o}{\rho c a} e^{-x/a} \tag{6}$$

as part of Eq. (5). As such, Eq. (6) represents the temperature rise in the sample near the surface of the material due to the flash. This is in accordance with Beer's law regarding attenuation of radiation in semitransparent substances. Just as the flash energy parameter is lumped into a parameter group, thermal conductivity cannot be specifically determined as part of the flash diffusivity experiments. It

Table 1 Four mathematical models used in analyzing the experiment

Model	Description	Parameters involved
(a)	Isotropic conduction and surface flash heating	$\alpha, Bi, q_o/\rho c L$
(b)	Anisotropic conduction and surface flash heating	$\alpha_a, \alpha_r, Bi, q_o/\rho c L, r_h$
(c)	Isotropic conduction and penetrating flash heating	$\alpha, a, Bi, q_o/\rho c L$
(d)	Anisotropic conduction and penetrating flash heating	$\alpha_a, \alpha_r, a, Bi, q_o/\rho c L, r_h$

is lumped into the Biot number (hL/k_a) and thermal diffusivities ($k_a/\rho c$ or $k_r/\rho c$). The Biot number is considered as another unneeded parameter, along with $q_o/\rho cL$, because q_o cannot be determined directly, but must be calculated in order to determine thermal diffusivity. The determination of the values for the two thermal diffusivity terms in the equations, α_a and α_r, is the sole objective of the experiment. All other parameters in the model are disposable, except to the extent to which they are needed to find the desired diffusivity values. In this work, the axial Biot number is used by convention, where the characteristic length is the thickness of the sample and the conductivity k_a is the thermal conductivity in the axial direction. Because the convection coefficient is assumed to be uniform over the surface, a radial Biot number could be computed from the axial Biot number by a straight proportion. However, only one Biot number is needed to facilitate the calculations, so the axial Biot number is used.

A primary difference between the present methods and the analysis method described in [1] is the use of a direct numerical temperature calculation of Eqs. (1)–(5), which are solved iteratively as they are matched to the measured data. Using the method of least squares, the model parameters are adjusted until a best fit is found, using the principles of [12]. Using this method, all parameters are adjusted in each model in order to achieve the best fit. As a general rule, the models with more parameters achieve a better fit. The legitimacy of the additional parameters can be verified statistically using the F test, as described Sec. IV. The residuals from this fit are examined to determine the adequacy of the fit of various levels of sophistication in the model to determine the most appropriate set of parameters to be used. The standard deviation σ of the residuals is calculated using Eq. (7):

$$\sigma = \sqrt{\frac{\sum_{i=1}^{n} (T_i - Y_i)^2}{n-1}} \tag{7}$$

In this equation, T_i and Y_i are the calculated and measured temperatures, respectively, on the surface of the material. This standard deviation is used as a quantitative means of comparison of the performance of the various models competing against one another. As part of this method, sensitivity coefficients are generated in adapting the best fit of the mathematical model to the measured temperature data. These sensitivity coefficients are simply partial derivatives of the calculated temperature with respect to each individual parameter.

The sensitivity coefficients are normalized by multiplying by the applicable parameter so that the sensitivity coefficients are all in units of temperature and their magnitudes can be compared directly. An example of the normalized sensitivity coefficient for radial diffusivity α_r is given in Eq. (8) next:

$$X_{\alpha_r} = \alpha_r \frac{\partial T}{\partial \alpha_r} \tag{8}$$

Figure 4 shows a plot of each of these sensitivity coefficients as functions of time. As can be seen in this figure, one sensitivity coefficient is calculated as a function of time for each of the six parameters being estimated. The six parameters being estimated as part of this modeling work are q_o the magnitude of the flash; α_a the axial diffusivity; α_r the radial diffusivity; a the penetration of the flash beyond the heated surface, which corresponds to the mean free path of a photon in the material; the Biot number; and r_h the heated radius of the sample surface. These sensitivity coefficients apply equally to the whole-surface measuring method and the single-point temperature method, because all six parameters are computed in both methods. All of the sensitivity coefficients are fairly large, with the exception of the radial diffusivity and the flash penetration depth. Still, convergence was obtained when estimating these parameters. This is true of both methods, including the method using a point measurement in the center of the sample and the method using the full-surface temperature history of the sample. The convergence criteria used were for the changes in parameters between iterations to be limited to 0.1% or less.

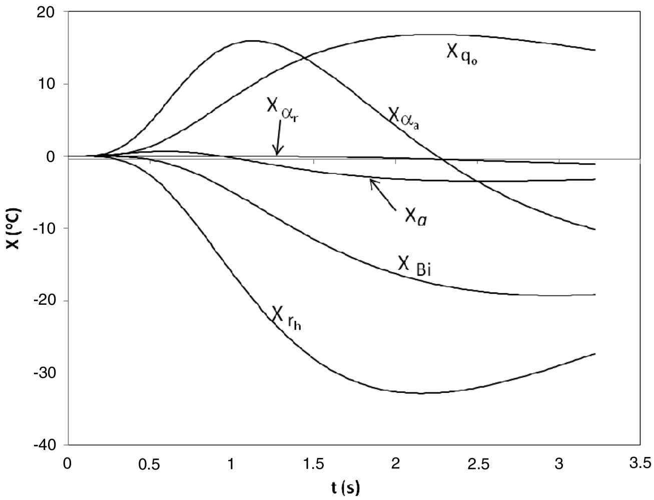

Fig. 4 Sensitivity coefficients for each of the six parameters used in the analysis.

IV. Results

As the mathematical models described in Table 1 become more sophisticated, the conformance of the model to the experimental measurements improves. Figure 5 graphically depicts the residuals from the single-point temperature measurement method. Table 2 provides a summary of the results from the four models. As can be seen in this table, as each level of sophistication is added to the model, there is a reduction in the standard deviation of the residuals. The residuals are simply the differences between the experimentally measured temperatures and the calculated temperatures from the model.

Using the statistical F test to compare the magnitudes of these residuals, as described in [12], it can be shown that model (d), as given in Table 1, the most sophisticated of the models used in this work, is the most valid of the four models compared. Moreover, the validity of model (d) is statistically significant at a 95% confidence level.

As an example of using this method, comparing models (c) and (d), the addition of the anisotropic parameter reduces the sum of squares of the errors between the two results by 3.032 °C^2. Dividing this number by the square of the standard deviation of the residuals in the higher-order model gives a value of 255.2 (dimensionless). This is significantly greater than 3.95, which is the value of the F statistic at a 95% confidence level for the number of degrees of freedom in this model. This outcome signifies that the addition of the anisotropic parameter is statistically significant at a 95% confidence level.

With model (d) providing the most adequate fit to the experimental measurements, it used in the comparison between the full-surface temperature measurement method and the single-point temperature measurement method. Table 3 shows the results for each of the six parameters using both the single-point measurement system and the measurement of the full surface using the thermal camera. As can be seen in this table, the results for the parameters of interest are within 7% of one another, regardless of the method used, specifically the axial and radial diffusivities. The diffusivity parameters are the only parameters of interest and the only reason the experiment is being conducted. The remaining parameters must all be estimated in order to optimize the fit of the theoretical model to the experimental measurements because all parameters in the model are interrelated and affect the temperature generated by the model. If, instead, values for some of the dispensable parameters were simply assumed, instead of being simultaneously calculated with the parameters of interest, the latter would be in error. However, the estimation of these additional parameters is not the objective of the experiment.

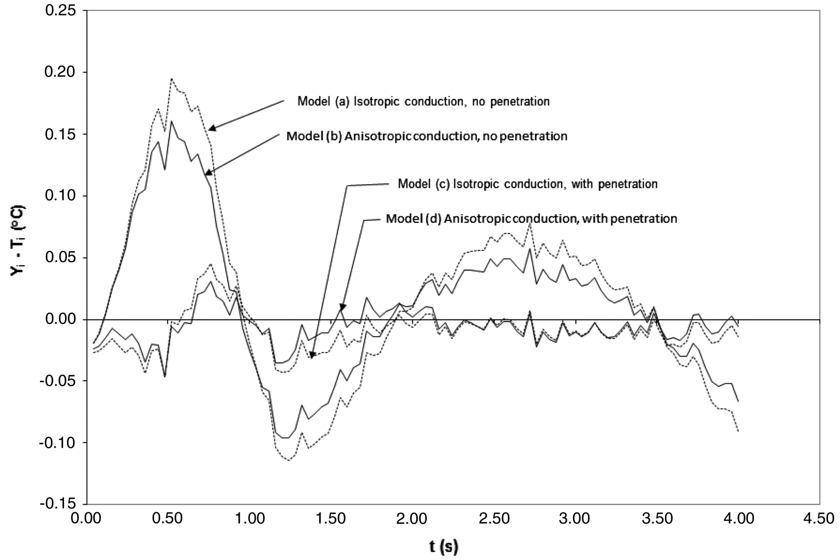

Fig. 5 Residuals for the single-point temperature measurement method.

By comparing the standard deviation of the residuals presented in Table 3 for the two methods, it would appear at first glance that the single-point measurement system produced superior results to those of the full-surface measurement system. The standard deviation of the residuals in the full-surface test is approximately five times that of the single-point case. However, Fig. 6, which shows a plot of the residuals with respect to time for the full-surface temperature measurement method, gives insight into part of the reason for this difference. Near the extreme edges of the sample, the temperature residuals are significantly larger than elsewhere across the sample. It is likely that radiation from the sample holder influences the temperature measurements near the perimeter of the sample. The sample holder is irradiated by the flash, to some extent, at the same time as the sample. Being made of steel, the sample holder has a higher diffusivity than the sample and the energy from the flash conducts more rapidly through the steel. It can be seen in Fig. 6 that the measured temperature at these edge points becomes quite a bit higher than expected for a brief period of time and then returns very close to the temperature predicted by the model. These points could have been removed from the measured data, but it was desired to retain the full width of the temperature measurements in order to be as objective as possible in analyzing the data.

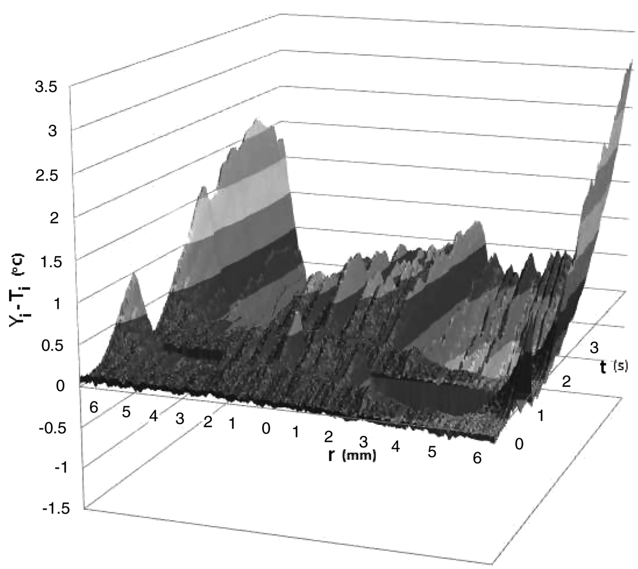

Fig. 6 Residuals for the full-surface temperature measurement method.

Table 2 Summary of results from analyzing one typical experiment using four different analysis models[a]

Model	α_a, mm^2/s	α_r, mm^2/s	Bi	a, mm	σ, °C
(a)	0.513	NA	0.629	NA	0.2103
(b)	0.509	1.015	0.631	NA	0.1814
(c)	0.497	NA	0.668	0.103	0.1661
(d)	0.482	1.652	0.650	0.119	0.1090

[a]Each model is successively more sophisticated, containing additional parameters, but generates improved results.

Table 3 Parameter estimation results and residuals

Parameter	Full-surface measurement	Single-point measurement
α_a, mm^2/s	0.448	0.482
α_r, mm^2/s	1.652	1.549
$q_o/\rho cL$, °C	15.675	19.967
Bi (dimensionless)	0.650	0.650
a, mm	0.118	0.119
r_h, mm	10.093	11.971
σ, °C	0.5404	0.1090

As an added check, a standard deviation of the errors in the temperature measurements was performed by comparing the radial symmetry of the measurements. Points along the line on which temperatures were measured on the back surface of the sample were compared at equal distances from the center of the sample. The mathematical model naturally calculates temperatures that are assumed to be radially symmetric; this is the expectation assuming uniform heating of the sample. However, the standard deviation calculated for the error in temperature measurements at equal distances from the center was found to be 0.4248°C. With this in mind, the standard deviation of the residuals between the mathematical model and the experimental measurements for this case of 0.5404°C is quite reasonable.

With these factors in mind, it is evident that the use of the full-surface measurement system offered little or no advantage to the estimation of parameters using only the single-point measurement system. The added complexity in performing the experiment, the postprocessing of the data, and applying a mathematical model with 201 temperature histories vs one temperature history is fairly significant. The use of the single-point measurement system seems to be a superior method for finding these orthotropic thermal properties when employing the flash method for diffusivity measurement, due to its comparable accuracy and reduced complexity. The variation of temperature at any one pixel near the center of the sample, when compared against the mathematical model, is on the order of 0.1 to 0.05°C. The spatial variation from one side of the sample to the other is much larger (nominally 0.5°C), which also adds to the liabilities of the full-surface measurement method.

V. Conclusions

Four mathematical models were used to analyze flash diffusivity data for a semiporous anisotropic material. The model allowing for flash penetration and nonuniform heating was shown to be the most adequate of these models at a 95% statistical confidence level. Using this model, two methods for computing anisotropic thermal diffusivity were compared in analyzing experiments performed using the flash method. One method used a single temperature history from a point in the center of the circular sample face. The other method used 201 temperature histories across the back of the sample, as measured by a thermal camera. The results using the two methods were very similar to one another and the mathematical models matched the experimental measurements in both cases, with residual standard deviations consistent with the anticipated measurement errors associated with each case. Some temperature anomalies were observed in the full-surface measurements near the perimeter of the cylindrical samples, presumably due to sample holder effects and slight unevenness in the flash diffusivity instrument. Considering these issues, and the added complexity introduced with the measurement and analysis of 201 temperature histories, as compared with one temperature history, the single-point method for determining anisotropic thermal diffusivities was found to be an adequate and preferable procedure.

Acknowledgment

This research at the Oak Ridge National Laboratory's High Temperature Materials Laboratory was sponsored by the U. S. Department of Energy, Office of Energy Efficiency and Renewable Energy, Vehicle Technologies Program.

References

[1] Parker, W., Jenkins, B. C., and Abbott, G., "Flash Method of Determining Thermal Diffusivity, Heat Capacity and Thermal Conductivity," *Journal of Applied Physics*, Vol. 32, No. 9, 1961, pp. 1679–1684.
doi:10.1063/1.1728417

[2] Cowan, R., "Pulse Method of Measuring Thermal Diffusivity at High Temperature," *Journal of Applied Physics*, Vol. 34, No. 4, 1963, pp. 926–927.
doi:10.1063/1.1729564

[3] Clark, L., and Taylor, R., "Radiation Loss in the Flash Method for Thermal Diffusivity," *Journal of Applied Physics*, Vol. 26, No. 2, 1975, pp. 714–719.
doi:10.1063/1.321635

[4] Koski, J., "*Improved Data Reduction Methods for Laser Pulse Diffusivity Determination with the Use of Minicomputers*," National Technical Information Service, Springfield, VA, 1981.

[5] Taylor, R., "Heat Pulse Thermal Diffusivity Measurements," *High Temperatures-High Pressures*, Vol. 11, 1979, pp. 43–58.

[6] Amazouz, M., Moyne, C., and Degiovanni, A., "Measurement of the Thermal Diffusivity of Anisotropic Materials," *High Temperatures-High Pressures*, Vol. 19, 1987, pp. 37–41.

[7] Graham, S., McDowell, D., and Dinwiddie, R., "In-Plane Thermal Diffusivity Measurements of Orthotropic Materials," *Thermal Conductivity*, Vol. 24, 1999, pp. 241–252.

[8] Cernuschi, F., Bison, P., Figari, A., Marinetti, S., and Grinzato, E., "Thermal Diffusivity Measurements by Photothermal and Thermographic Techniques," *International Journal of Thermophysics*, Vol. 25, No. 2, March 2004, pp. 439–457.
doi:10.1023/B:IJOT.0000028480.27206.cb

[9] Kruczek, T., Adamczyk, W., and Bialecki, R., "In-Situ Measurement of Thermal Diffusivity in Anisotropic Media," *International Journal of Thermophysics*, Vol. 34, No. 3, 2013, pp. 467–485.
doi:10.1007/s10765-013-1413-3

[10] Czichos, H., Saito, H., and Smith, L., *Handbook of Material Measurements*, Springer–Verlag, Heidelberg, Germany, 2006.

[11] McMasters, R., Beck, J., Dinwiddie, R., and Wang, H., "Accounting for Penetration of Laser Heating in Flash Thermal Diffusivity Experiments," *Journal of Heat Transfer*, Vol. 121, No. 1, 1999, pp. 15–21.
doi:10.1115/1.2825929

[12] Beck, J., and Arnold, K., *Parameter Estimation*, Wiley, New York, 1977.

Queries

1. AU: Please check that the copyright (©) type is correct. Please note that the code will be added upon publication.

2. AU: Instructions from AIAA indicate that all figures are to appear in color only online. Please verify the usage of color in your proof is correct, and note that all figures will be grayscale in the print journal.

3. AU: Please provide page range for Refs. [4, 10, 12].

4. AU: Please provide an issue number for Refs. [5–7].